

106

Hydrologic and Paleohydrologic Assessment of the 1993 Floods on the Verde River, Central Arizona

by

P. Kyle House, Philip A. Pearthree, and Jonathan E. Fuller'

Arizona Geological Survey
Open-File Report 95-20

December 1995

Arizona Geological Survey
416 W. Congress, Suite #100, Tucson, Arizona 85701

JE Fuller/ Hydrology and Geomorphology, Inc.

*Contribution #46 from the Arizona Laboratory for
Paleohydrological and Hydroclimatological Analysis (ALPHA)*

*Research funded by the Salt River Project, the Hydrological Sciences Program of the
National Science Foundation, and the Arizona Geological Survey*

This report is preliminary and has not been edited
or reviewed for conformity with Arizona Geological Survey standards

Abstract

The Verde River experienced very large floods in January and February of 1993 during a major episode of flooding that affected most of the large drainages in Arizona. The January flood peak discharge on the lower Verde River ($4,100 \text{ m}^3 \text{ s}^{-1}$) was the largest of the gage record, and the February flood peak ($3,650 \text{ m}^3 \text{ s}^{-1}$) was the second largest. These large, very recent floods provide an exceptional opportunity to investigate the genesis of large floods on the Verde River, to compare the sizes of the 1993 floods with other large historical and prehistoric floods, and to evaluate the fidelity with which slackwater deposits and other paleostage indicators reflect the peak water surface.

The complex flood hydrology of the Verde River is illustrated by the floods of 1993. The 1993 floods were generated by a series of global- and regional-scale climatic events. Warm sea-surface temperatures associated with El Niño-Southern Oscillation conditions developed during the winter of 1993. The Pacific storm track split; the southern branch combined with the subtropical jet stream to direct numerous wet storms into Arizona, which led to saturation of drainage basins throughout the region. The large floods on the Verde River were further enhanced by snowmelt induced by rainfall as relatively warm storms passed through after cold storms. The geometry of the elongate Verde basin is also an important factor affecting the genesis of large floods. The upper $5,500 \text{ km}^2$ of the Verde basin above the Paulden gage contributed minimal flow to the January and February peaks on the lower Verde River because the flood peaks from the upper basin lagged far behind the peaks in the central and lower basin. The central Verde basin above the Camp Verde gage (about $6,500 \text{ km}^2$) was responsible for only about one-third of the January peak on the lower Verde River. There was a tremendous increase in the flood peak between Camp Verde and Tangle Creek (about $2,000 \text{ km}^2$ increase in drainage area). In the February flood, more than 95 percent of the flood peak discharge recorded at Tangle Creek originated above the Camp Verde gage. Other historical floods of the Verde River had hydrologic characteristics between the extremes of the 1993 floods.

We evaluated the uncertainties associated with the use of various types of peak water surface indicators in hydraulic modeling and flow reconstruction using 1993 flood deposits. We surveyed channel geometry and various high-water indicators along a 500-m-long reach of the lower Verde River near Red Creek that had previously been studied in the 1980s. Tops of typical slackwater sedimentary deposits in this relatively steep-sided reach are 1 to 2 m below the peak water surface as indicated by floated debris, resulting in a ~30 percent underestimation of the peak discharge. In a more cursory evaluation of another reach downstream where the confining topography is quite gentle, we found that tops of slackwater deposits are about 30 cm below the peak water surface, resulting in a 5 to 10 percent underestimation of the peak discharge.

Paleoflood estimates for the 1993 flood peak discharge and older floods can be reconciled with the gage record. Our best estimate for the peak 1993 discharge at Red Creek ($3,450 \text{ m}^3 \text{ s}^{-1}$) is substantially less than that obtained at the Tangle Creek gage about 10 km downstream ($4,100 \text{ m}^3 \text{ s}^{-1}$). This discrepancy likely is real, and not caused by modeling uncertainty. The January peak increased tremendously between Camp Verde and Tangle Creek, whereas the February peak increased very little. The rates of increase downstream were such that the February peak was probably the largest discharge at Red Creek. Previous paleoflood estimates for other large historical floods are quite consistent with each other and with the gage record after they have been adjusted upward based on the relationships obtained for the 1993 floods. Based on flood deposit stratigraphy, we propose that the flood of 1891 was slightly larger than the largest 1993 flood at Red Creek. We also found evidence for two substantially larger floods that probably occurred at least 1,000 years ago. The largest of these may have had a peak discharge of $5,000$ to $5,500 \text{ m}^3 \text{ s}^{-1}$ at Red Creek. Incorporating these data into the MAX program of Stedinger and others (1986), we estimate a Q100 of $4,020 \text{ m}^3 \text{ s}^{-1}$ and a Q500 of $5,350 \text{ m}^3 \text{ s}^{-1}$. These are reasonably consistent with previous estimates, but are far less than probable maximum flood estimates for the Verde River.

Introduction

The Verde River experienced very large floods in January and February of 1993. These floods were part of a major episode of flooding during the winter of 1993 that affected most of the large drainages in Arizona. The January flood peak discharge on the lower Verde River was the largest since 1891, and the February flood peak was the second largest. Many gaged sites on the middle and upper Verde River and its tributaries measured record peak discharges as well (see figure 1 and table 1 for summary). Based on previous paleohydrological analyses conducted on the lower Verde River, the 1993 floods were comparable to the magnitudes of the largest historical floods, but were smaller than the largest floods of the past 1,000 years (Ely and Baker, 1985, O'Connor and others, 1986).

The 1993 floods serve as useful analogs to large paleofloods because of their interesting hydrological characteristics and the abundant geomorphic evidence left in their wake. Previous paleoflood studies conducted in Arizona, including the lower Verde River, primarily used flood slackwater deposits (SWD) as evidence of the peak water surface. These features are known to provide only a minimum estimate of the water surface, and the amount that they fall short of the peak stage and the resultant underestimation of discharge are not well known. Examination of abundant, clear evidence of the maximum 1993 flood stage at two sites on the river enabled us to develop a relation between the heights of SWD and definitive peak stage indicators (flotsam) and thus augment the paleoflood record. Post-flood field investigations and examination of hydrological data also revealed some important characteristics of the flood hydrology of the Verde River basin that are useful in interpreting the paleoflood record.

Two paleoflood studies were conducted on the lower Verde River prior to the 1993 floods. Ely and Baker (1985) studied a reach approximately 6 km upstream of the gage near Tangle Creek (TC), which will be referred to as the "Ely-Baker reach" (figure 2). They estimated peak discharge estimates for two recent floods that were comparable to estimates from the gage, implying that their modeling was good. They also reported an estimate of the discharge of the 1891 flood (the historical peak of record) and described a substantially larger flood that occurred approximately 1,000 years BP O'Connor et al (1986) studied a site above the mouth of Red Creek approximately 6 km upstream of the Ely-Baker reach (figure 2). This site will be hereafter referred to as the "Red Creek reach". The goal of their study was to check for consistency between the paleoflood records at each site. They concluded that the record from the Red Creek site was incomplete and the discharge estimates from correlative deposits were significantly lower than at the Ely reach.

In this report we summarize the results of a post-flood investigation of the 1993 floods on the Verde River. We occupied and restudied sites of the two previous paleohydrological investigations. Our principal

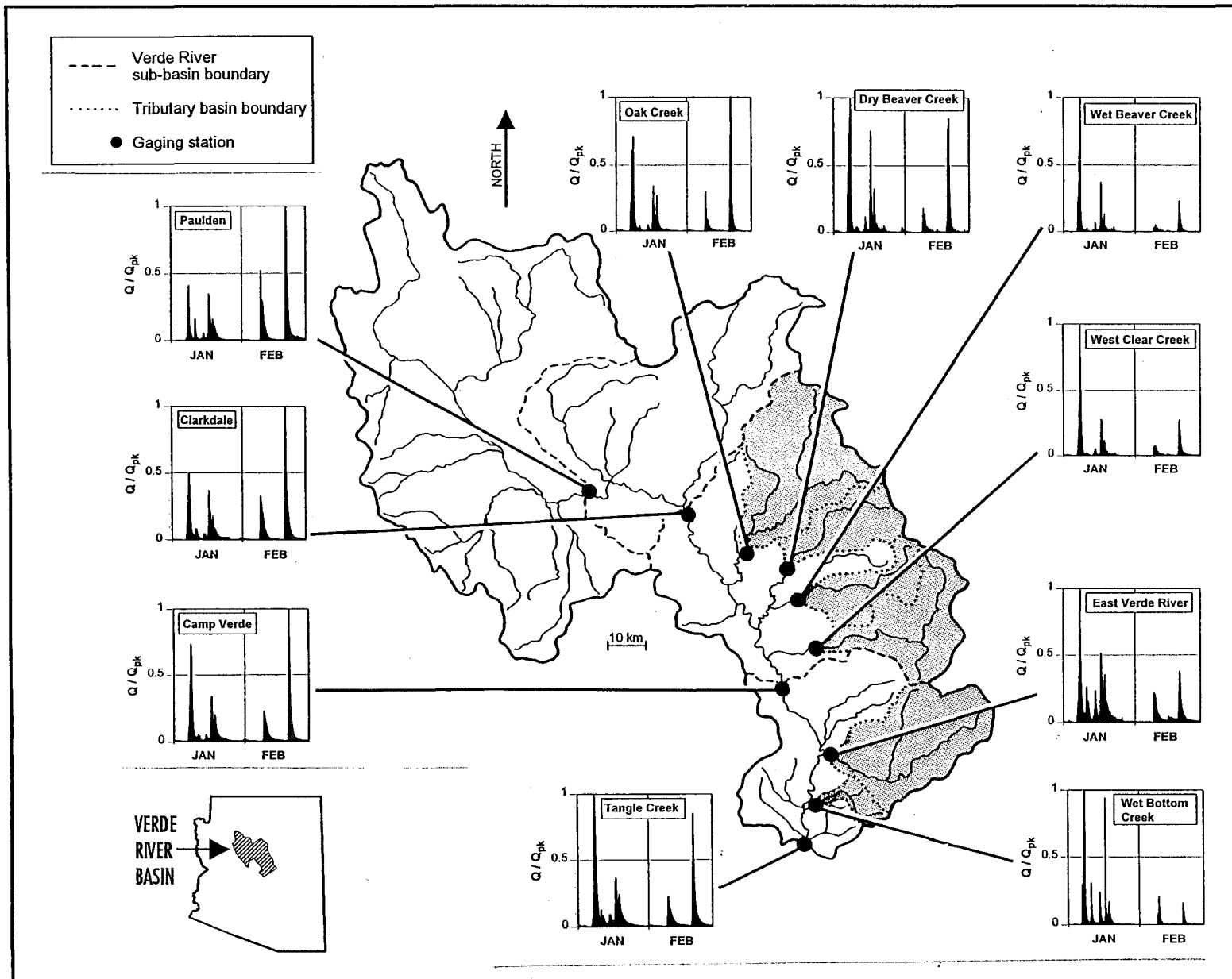


Figure 1. Map of the Verde River basin above Tangle Creek gage. Unit hydrographs for January and February, 1993, show the relative sizes of the various flood peaks at each gage site. Shading indicates the drainage area accounted for by gages on the tributaries of the Verde River.

Site	January 8, 1993 Qpk	Time	January 17, 1993 Qpk	Time	February 9, 1993 Qpk	Time	February 20, 1993 Qpk	Time
Verde nr Paulden	257	19:30	217	15:00	326	8:00	657	9:45
Verde nr Clarkdale	745	13:00	558	7:00	498	1:45	1507	4:00
Oak Creek	524	11:45	251	5:15	222	2:45	736	3:30
Dry Beaver Creek	329	9:15	249	3:15	61	0:45	280	5:15
Wet Beaver Creek	453	6:30	169	6:00	25	18:30	107	1:30
West Clear Creek	702	8:00	198	6:00	56	19:00	195	1:00
Verde blw Camp Verde	2478	13:00	1150	12:30	782	10:45	3370	11:00
East Verde River	569	7:00	295	7:45	127	7:15	217	2:45
Wet Bottom Creek	209	7:00	197	7:30	44	15:30	34	5:45
Verde blw Tangle Ck	4106	8:30	1509	18:30	952	16:00	3512	16:00

Table 1. Summary of the magnitude and timing of peak discharges of 1993 floods at gaging stations in the Verde River basin.

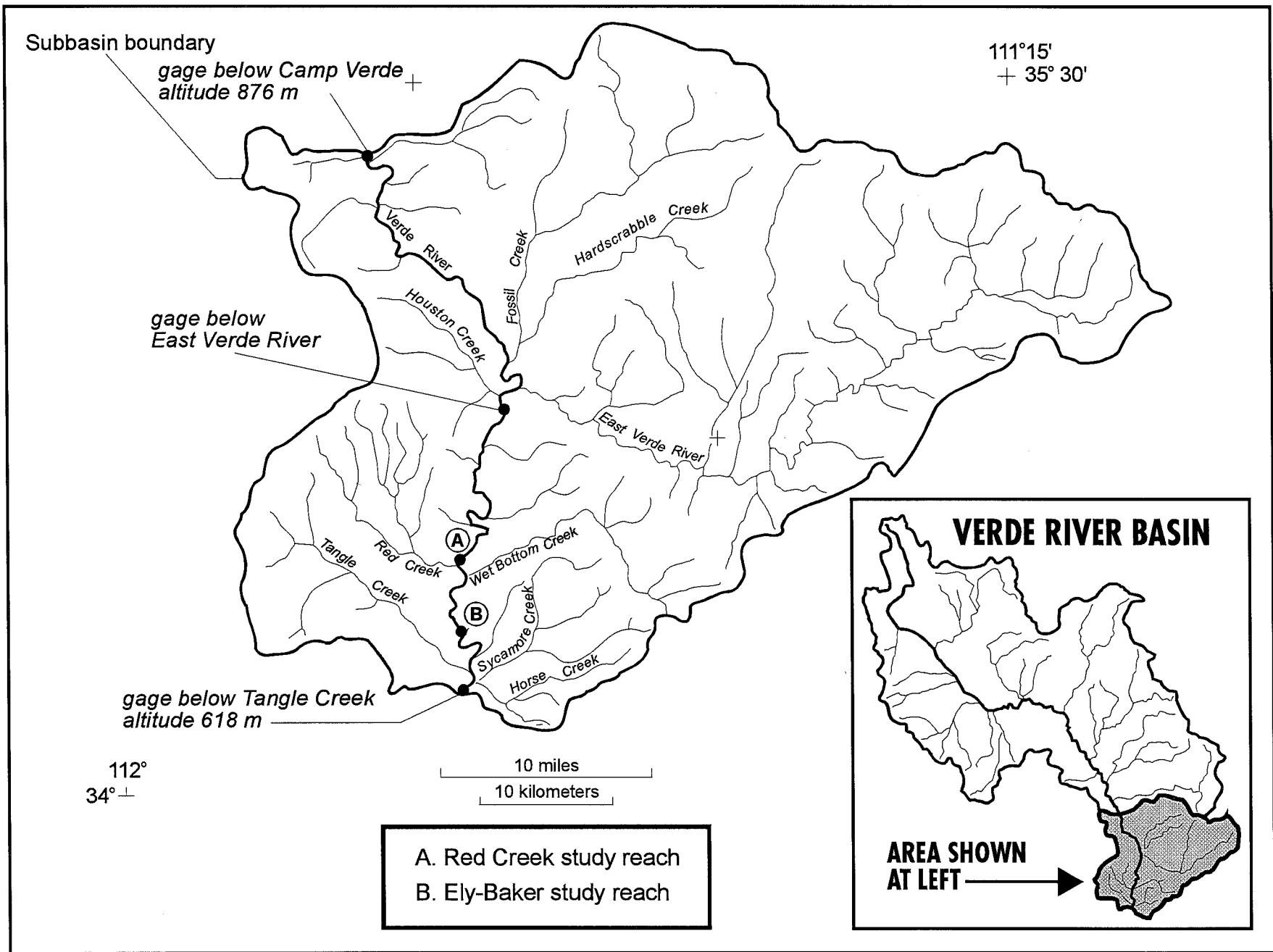


Figure 2. Detailed map of the lower Verde River basin. Paleoflood study sites are identified.

objectives were to: (1) estimate the peak 1993 flood magnitude at each site through analysis of gaged data and by fitting the results of hydraulic modeling to diagnostic peak stage indicators; (2) quantify the relation between discharge estimates from different indicators of flood stage, in particular SWD and flotsam; (3) revise previously reported paleoflood discharge estimates from each site in light of the results of (2); (4) attempt to reconcile or explain discrepancies among discharge estimates reported from the two paleoflood study sites and the gages; and (5) re-evaluate long-term flood magnitude-frequency relationships through flood frequency analysis of the composite data set of the revised paleoflood discharge estimates and the historical and systematic flood data.

Hydroclimatology of the 1993 Arizona Floods

The 1993 winter flooding in Arizona was the greatest and most widespread occurrence of regional flooding in the state since at least 1891 (House and Hirschboeck, 1995). Record precipitation totals resulting from an anomalously high frequency of frontal storm passages caused extreme flooding on the Verde River and throughout much of Arizona in January and February 1993. The fronts were steered over the state by an exceptionally active storm track that was located unusually far south. Frontal precipitation was frequent and heavy over much of the state; precipitation in the mountainous terrain of central Arizona where much of the Verde River drainage basin is located was particularly heavy.

The flooding ultimately resulted from a series of global- and regional-scale climatic events and hydrologic conditions that transpired prior to and during the January/February flooding episode (*cf.* House and Hirschboeck, 1995, for detailed discussion). A key component of the flooding episode was an unusually strong large-scale atmospheric circulation anomaly that developed over the eastern Pacific Ocean and persisted throughout the winter of 1992/93. El Niño-Southern Oscillation (ENSO) conditions developed during December 1992 and lasted through February 1993. As a consequence, above-normal sea surface temperatures (SSTs) expanded eastward in the tropical and subtropical Pacific Ocean, and the winter of 1992/93 marked one of the longest periods of continuous warm SSTs on record for the tropical Pacific. The atmospheric circulation accompanying this SST anomaly was an enhanced subtropical jetstream that conveyed warm, moisture-laden air from the tropical Pacific to the southwestern United States. Also, an anomalous high pressure area developed in the Gulf of Alaska in December and persisted through the winter. This high pressure system displaced one branch of the Pacific storm track far to the north and another branch to the south, where it combined with the enhanced subtropical jetstream. This split-flow configuration led to above-normal cyclonic storm activity moving into the southwestern United States.

Interaction between the subtropical and extratropical flow configurations resulted in a long succession of alternating cold and warm storms passing over the southwest United States from early December 1992 through February, 1993. This ultimately led to nearly complete saturation of drainage basins throughout the region. Precipitation from storms in January and February therefore immediately generated surface runoff. Furthermore, the alternating passage of cold and warm storms led to a sequence of events whereby snow accumulation and subsequent snowmelt, enhanced by rain falling on the snow, greatly augmented the amount of runoff. This combination of phenomena led to the extreme flooding on the Verde River and on rivers and streams throughout much of Arizona during January and February, 1993.

Characteristics of the Verde River Basin

The Verde River basin includes slightly more than 14,000 km² of central Arizona. Four continuous recording gages are located along the river and on six of its tributaries (figure 1). The uppermost gage on the Verde is near Paulden, AZ. Its contributing drainage area is 5,568 km², which is about 40% of the total basin area. Despite its large size, this portion of the basin contributes little to no runoff to the peak discharges of large floods recorded at the gages downstream. Flood peaks recorded at Paulden almost always follow those at the next gage downstream by several hours. This lag is probably due to the elongated shape of the upper basin, circuitous drainage routes, and minor storage effects of a small lake just upstream of the gage (Chin and others, 1991). Downstream, the next gage is near Clarkdale, Arizona. Its contributing drainage area is 8,148 km², accounting for about 60% of the total basin area but only 30% of effective flood peak-producing area (i.e. the area below the gage at Paulden). The next gage downstream of Clarkdale is near Camp Verde, Arizona. Its contributing drainage area is 12,028 km², which is 85% of total basin area and 75% of the flood-peak producing area. Between Clarkdale and Camp Verde, four relatively large, gaged tributaries enter the Verde River: Oak Creek (920 km²), Dry Beaver Creek (368 km²), Wet Beaver Creek (288 km²), and West Clear Creek (624 km²) (see figure 1). They account for about 55% of the drainage area between the Clarkdale and Camp Verde gages. The lowermost gage on the unregulated portion of the Verde River basin is located below Tangle Creek. It records runoff from a total of 14,227 km², including an additional 2,200 km² below the CV gage. Only two tributaries in this portion of the basin are gaged: the East Verde River (857 km²) and Wet Bottom Creek (94 km²) (figure 2).

Hydrology of the 1993 floods in the Verde River Basin

The timing of peak discharges at the gages in the Verde River basin during the winter of 1993 reflects the role of different portions of the basin in contributing to the peak runoff (figure 1 and table 1). Many gaged floods on the Verde River have exhibited very consistent flood-peak travel times between the various gages. For example, Aldridge and Hales (1985) concluded that the travel time of floods between the Camp

Verde (CV) and Tangle Creek (TC) gages is typically 6 hours based on characteristics of several recorded flood events. The flood of February 20, 1993, provides an excellent measure of travel time of a large peak discharge between these sites. Gage data indicates that almost all of the runoff (> 95%) in this event originated upstream of CV. The flood peak took almost exactly 5 hours to travel between the gages. Combining this with the 6 hour figure previously cited, we will assume that 5.5 hours is a reasonable average measure.

In the January 8 flood, the peak discharge at TC occurred 4.5 hours before the peak discharge at CV, indicating that much of the January 8 flood peak at TC was derived from the lower Verde basin. The peak discharge of $4106 \text{ m}^3 \text{ s}^{-1}$ (145,000 cfs) at TC was recorded at 8:30 AM on January 8 (see table 1); the discharge recorded at CV 5.5 hours prior to this was approximately $1416 \text{ m}^3 \text{ s}^{-1}$ (50,000 cfs). Thus the portion of the basin between the gages contributed an immense quantity of runoff to the peak (approximately $2690 \text{ m}^3 \text{ s}^{-1}$ [95,000 cfs], or 66% of the peak), which progressively increased as the flood wave traveled through the lower basin.

The unusual timing of the early January peaks recorded at CV and TC arose from a chance combination of hydrologic events in the middle basin (i.e. the area between Paulden and Camp Verde) and lower basin (i.e. the area below Camp Verde). Hydrographs from gaged tributaries show that two distinct pulses of peak runoff characterized the early January event (figure 3). The second peak is greater than the first peak in both the middle and lower portions of the basin, but their relative difference is greater in the lower basin than in the middle basin. From this relation we conclude that the exceptionally large peak recorded at TC resulted from the coincidental, nearly optimal combination of the first peak from the middle basin with the second peak from the lower basin. The subsequent peak at CV of $2475 \text{ m}^3 \text{ s}^{-1}$ (87,500 cfs) at 1:00 PM, January 8 contributed to the sustained high flow recorded at TC for most of the day. This situation illustrates the possibility that considerably different flood magnitudes may arise given slight variations in the timing of runoff initiation in different portions of the basin. This fact has important implications for the flood hydrology of the Verde River basin.

Independent Constraints on Peak Discharge at the Red Creek Site

Our primary post-flood study was carried out in a reach of the Verde River immediately above the mouth of Red Creek between CV and TC (figure 2). There is uncertainty about which flood had the largest peak in this reach because of the very different hydrological characteristics of the two large 1993 floods on the lower Verde River. The following discussion outlines reasoning that we used to constrain the peak discharges of the January and February floods through the Red Creek reach and thereby determine which of the two was most likely to have been the larger at the site. Our analysis relied on data from the gaging

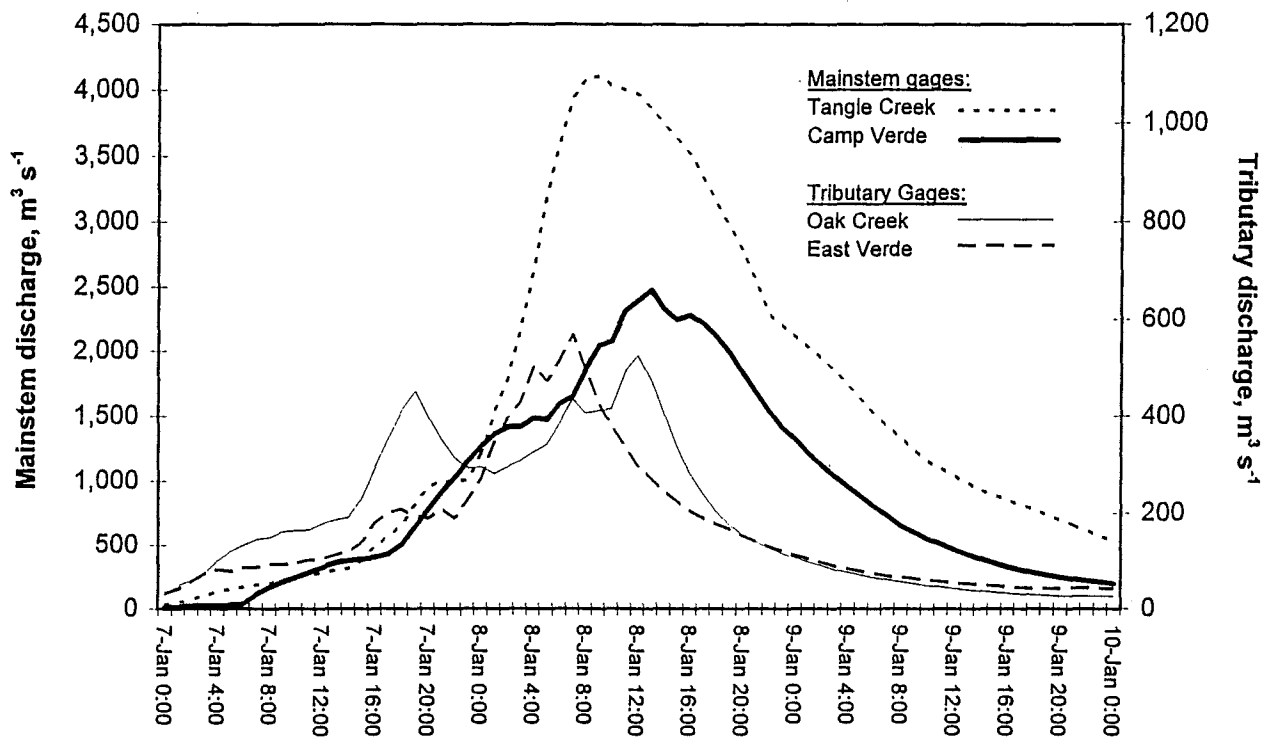


Figure 3. Hydrographs for the January flood from the Oak Creek and East Verde River tributary gages and the Camp Verde and Tangle Creek mainstem gages.

stations, and an independent peak discharge estimate from the Ely-Baker paleoflood study reach between Red Creek and TC.

The Early January Flood The early January peak increased by approximately $2,690 \text{ m}^3 \text{ s}^{-1}$ (95,000 cfs) between CV and TC, indicating that tributary inflow in the intervening drainage area was very large. Only two additional, gaged measures of the inflow are available. The East Verde River (drainage area of 857 km^2 ; see table 2 for summary of subbasin drainage areas and discharges), the largest tributary between the gages, recorded a peak of $570 \text{ m}^3 \text{ s}^{-1}$ (20,100 cfs) between 7 and 8 AM. Wet Bottom Creek (drainage area 94 km^2) recorded a record peak of $209 \text{ m}^3 \text{ s}^{-1}$ (7,380 cfs) at 7 AM. The peak of $4,106 \text{ m}^3 \text{ s}^{-1}$ at the TC gage was recorded at 8:30 AM, and the peaks on the two gaged tributaries were nearly synchronous with the passage of the peak down the mainstem. It is likely that most ungaged tributaries in the lower basin followed a similar trend and can easily account for the additional $1,910 \text{ m}^3 \text{ s}^{-1}$ (67,520 cfs). Principal sources of the inflow from this area include Fossil, Hardscrabble, Houston, Red, Tangle, and Sycamore creeks (figure 2). We know from post-flood field observations that Red, Tangle, and Sycamore creeks all experienced large floods in 1993 and we believe it is reasonable that, like Wet Bottom Creek, the largest flows occurred in early January and had timing consistent with the mainstem peak.

We use measures of unit runoff (i.e. discharge \div area) in combination with gage data to establish constraints on the peak discharge through the Red Creek reach (RC). We observed that Horse Creek basin, a small drainage (32 km^2) just upstream from the TC gage, was severely backflooded due to the influence of a bedrock constriction on the Verde and contributed little to no runoff to the peak. Thus, its drainage area is not included in calculating unit discharges for relevant subbasins. The absolute range of the early January peak through the Red Creek reach is $1,416 \text{ m}^3 \text{ s}^{-1}$ to $4,106 \text{ m}^3 \text{ s}^{-1}$ (50,000 to 145,000 cfs) based on the likely genesis of the largest peaks between CV and TC (figure 4). CV ultimately recorded a peak of $2,478 \text{ m}^3 \text{ s}^{-1}$ (87,500 cfs) at 1 PM that afternoon, however, which places a higher minimum constraint on the peak discharge through the RC. Better upper and lower bounds can be established using the peak discharges from Wet Bottom Creek (WBC) and the TC gage. A maximum of $3,900 \text{ m}^3 \text{ s}^{-1}$ (137,620 cfs) results from the difference between the WBC peak and the TC peak. This is an absolute maximum, however, because it assumes no input from Red, Tangle, and Sycamore creeks. A more realistic maximum constraint of $3,440 \text{ m}^3 \text{ s}^{-1}$ (121,500 cfs) results from the difference between the TC peak and the unit discharge of the area between CV and TC ($2,200 \text{ km}^2$) applied to the area between TC and RC. We consider this a maximum because it assumes a relatively low value of unit runoff for this size drainage area. In contrast, if the considerably higher unit discharge from WBC is applied to the smaller area between

	Site Name	Contributing Area (km ²)	Discharge (m ³ /s)	Unit Discharge (m ³ /s/km ²)
Gages	Verde River near Camp Verde (CV)	12,028	1,416	0.12
	Verde River below Tangle Creek (TC)	14,227	4,106	0.29
	East Verde River	857	569	0.66
	Wet Bottom Creek	94	209	2.22
Paleoflood Reaches	Red Creek (RC)	13,683	-	-
	Ely-Baker (EB)	13,932	3,682	0.26
Miscellaneous Sites	Red Creek	128	-	-
	Horse Creek	32	-	-
Sub-Basins	CV-TC	2,167	2,690	1.24
	TC-EB	264	425	1.61

Table 2. Contributing areas, peak discharges, and unit discharges for the January flood at various sites in the lower Verde River basin.

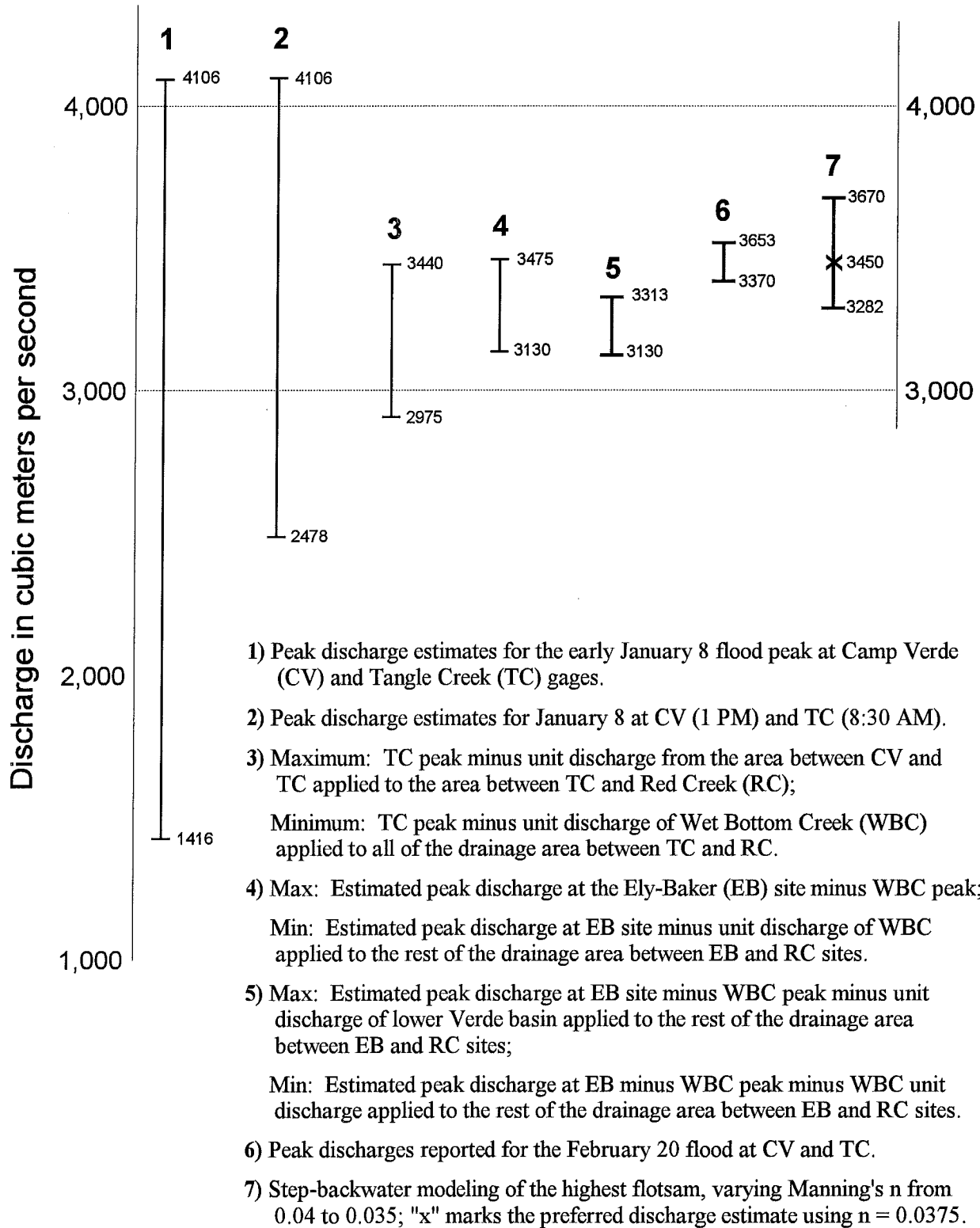


Figure 4. Constraints on the peak 1993 discharge at the Red Creek study reach.

TC and RC, then a likely minimum discharge estimate of $2,975 \text{ m}^3 \text{ s}^{-1}$ (105,000 cfs) results. Thus, using only the gage data, the estimated range for the January discharge through RC is $2,975$ to $3,440 \text{ m}^3 \text{ s}^{-1}$.

We obtained an independent estimate from the Ely-Baker reach that can be used to further constrain the discharge at the Red Creek site. At this site we estimated the 1993 flood peak discharge as $3680 \text{ m}^3 \text{ s}^{-1}$ (130,000 cfs) by reoccupying a cross section (section 9) and comparing the elevation of flotsam to stage-discharge relations reported in Ely (1985) and Ely and Baker (1985). In their study they reported an estimate for the 1980 flood discharge that was consistent with the gage estimate (i.e. within 1%), thus we assume that our estimate for the 1993 peak from this reach is reasonably good. Since the Ely-Baker site is located below the mouth of Wet Bottom Creek the difference between their peak discharges, $3,475 \text{ m}^3 \text{ s}^{-1}$ (122,620 cfs), is a reasonable maximum bounding value. Again, we claim that this is a maximum because it assumes no input from Red Creek which also enters the river between the study sites. A minimum of $3,130 \text{ m}^3 \text{ s}^{-1}$ (110,540 cfs) results from the difference between the Ely-Baker estimate and the unit discharge of WBC applied to the area between the Ely-Baker and Red Creek sites (249 km^2). This range can be narrowed further by limiting the application of unit discharges to only the Red Creek basin (128 km^2). An upper limit of $3,313 \text{ m}^3 \text{ s}^{-1}$ (117,000 cfs) results from applying the unit discharge of the area between CV and TC; and a lower limit results from applying the Wet Bottom Creek unit discharge. We conclude that the peak discharge of the January flood through the Red Creek reach was probably between $3,130$ and $3,313 \text{ m}^3 \text{ s}^{-1}$.

The Late February Flood. In the late February flood, peak discharge on the Verde River increased from $3,370 \text{ m}^3 \text{ s}^{-1}$ at CV to only $3,653 \text{ m}^3 \text{ s}^{-1}$ at TC, so approximately 95% of the peak originated upstream of the CV gage. This indicates that the February peak through the Red Creek reach has a lower limit ($3,370 \text{ m}^3 \text{ s}^{-1}$) greater than the upper limit of the likely range of the January peak discharge ($3,313 \text{ m}^3 \text{ s}^{-1}$) (figure 4). Thus, we conclude that the February flood was probably the larger peak through the Red Creek reach. The tremendous increase in the discharge of the early January flood in the lower basin was such that the peak discharge was less than the February peak through a significant length of the river between CV and TC, but was $565 \text{ m}^3 \text{ s}^{-1}$ (20,000 cfs) larger by the time it reached TC. The Red Creek reach is probably just upstream of the cross-over point where the two peaks were the same. Because both Red and Wet Bottom creeks enter the Verde between the Red Creek and Ely-Baker reaches, the January flood was probably larger than the February flood in the latter reach.

In our field investigations we did not note any conclusive evidence for the passage of two floods through the Red Creek reach, suggesting that evidence from the first flood was obscured by the second,

slightly larger flood. Evidence of two floods at the Ely-Baker reach is subtle because the peak stage of the January flood was probably less than 30 cm higher than the February flood. This small difference should have resulted in the flotsam from the February flood being deposited on the surface of January flood sediment. We observed this relationship in the field, but at that time we interpreted it to be the result of deposition during recession of the January peak.

Paleoflood Methodology

Paleoflood hydrology generally refers to the study of floods that occurred in the absence of instrumental observation or historical documentation (Baker, 1987, 1989). However, the term is also appropriate for the application of the same methodological procedures to studies of modern or historical floods (e.g. House and Pearthree, in press). A primary value of paleoflood studies is the extension of flood records by hundreds to thousands of years. Documentation of the actual occurrences of extreme floods over this time frame has important applications to studies of climatic variability (Ely and others, 1993), long-term flood magnitude-frequency characteristics (O'Connor and others, 1994), and potential bounds on flood peak magnitudes (Enzel and others, 1993).

In our study, we used the slackwater deposit-paleostage indicator (SWD-PSI) method of paleoflood reconstruction because it has proven to produce the most accurate estimates of paleoflood magnitudes (Baker, 1989). The SWD-PSI method estimates peak discharge through comparison of relict high-water indicators (SWD and PSI) to water-surface profiles generated from a step-backwater model such as HEC-2 (Hydrologic Engineering Center, 1985). The method is best suited for bedrock canyons or otherwise stable channels which are conducive to long-term preservation of flood evidence that retains a direct relation to the pre-flood and post-flood channel geometry (Baker and Kochel, 1988). Also, stable channels are generally more realistically characterized in hydraulic modeling. In a typical SWD-PSI study a range of discharges is reported from a visual assessment of the best overall agreement between the model-predicted profile and the relict high-water indicators (O'Connor and Webb, 1988).

Slackwater deposits (SWD) are sedimentary flood deposits usually consisting of silt, sand, and occasionally gravel that accumulate in areas of reduced flow velocity during floods (Kochel and Baker, 1988). SWD provide minimum estimates of the associated peak flood-stage because they are deposited at some depth below the peak water surface. Paleostage indicators (PSI) include a variety of non-sedimentary types of flood evidence, including: flotsam, scars on vegetation, erosion marks on canyon walls, flood-related vegetation distributions, and evidence for non-inundation. The relation between the elevation of a PSI and the associated peak flood-stage is variable and depends on the nature of the indicator. For example, highest flotsam commonly corresponds closely to peak stage, but flood scars on vegetation and/or canyon

walls, and massive piles of flood debris vary in their relation to peak stage. More detailed explanations of the SWD-PSI method can be found in: Baker (1987); Kochel (1988); Kochel and Baker (1988); O'Connor and Webb (1988); and Baker (1989).

The SWD-PSI method is similar to other indirect methods of estimating peak discharges of recent floods (e.g. Benson and Dalrymple 1967; Dalrymple and Benson, 1967). An important difference, however, is the use of step-backwater modeling instead of the slope-area method, which is commonly used in indirect estimates of recent large floods at ungaged sites and extension of rating-curves at gaged sites. The different choice of models reflects uncertainties inherent in the paleoflood evidence. Slope-area modeling requires a water-surface profile specified by high-water marks (e.g. flotsam), channel geometry, and energy-loss coefficients to calculate the discharge. In contrast, the step-backwater method treats discharge as a known value and uses it in conjunction with channel geometry and energy-loss coefficients to calculate the water-surface profile. This method is a logical choice for paleoflood studies where the true water-surface profile is often not precisely known from the basis of the relict stage indicators, but the channel geometry is reasonably well-constrained. In our re-study of the Verde River, even though definitive peak stage indicators were present, we used step-backwater modeling to facilitate comparison with previous studies and evaluate uncertainties in paleoflood reconstructions in general.

Limiting assumptions of the SWD-PSI method are associated with the flow model and its application in the context of paleoflood hydrology. Principal assumptions include: (1) flow is steady, gradually varied, and one dimensional; (2) channel cross-section boundaries are stable; (3) energy slope is uniform between cross-sections; (4) cross-section characteristics and the estimated energy loss coefficients are representative of those affected by the flood(s) in question; (5) PSI approximate the stage of the flood(s) in question—slackwater deposits represent a minimum peak flood-stage, but other types of paleostage indicators may represent the peak water surface (flotsam), or provide a maximum bound on the peak stage (e.g. some flood scars, or evidence of non-inundation); and (6) either a negligible amount of scour or deposition has occurred in the channel during and since the flood peak, or any that occurred can be accounted for in some way (modified from O'Connor and Webb, 1988; Hoggan, 1989; and Baker, 1989). These assumptions apply to most types of indirect discharge estimation, but their relative importance increases with the amount of time between the occurrence of the flood(s) and the reconstruction attempts. Focusing modeling efforts in stable channels helps to minimize the violation of some of the assumptions and the effects of time-variant changes in channel geometry.

Field Investigations

In our study following the 1993 floods, we resurveyed a 500-m-long stretch of the Verde River that constitutes the lower third of the Red Creek reach studied previously by O'Connor and others (1986). Our field investigation was performed in June, 1993, approximately 4 months after the flooding. The study reach is in a relatively wide canyon with steep to nearly vertical walls. Bedrock protrudes from the bed at several places along the canyon bottom, elsewhere, the bottom is composed of a pool and riffle sequence with an average slope of about 1 percent. Much of the canyon bottom area above the perennial low flow channel consists of a nearly flat boulder and cobble bar. The alluvial cover throughout the reach is probably thin; however, depth to bedrock was not determined quantitatively.

Our study reach consists of nine cross sections within a 500-m-long stretch of the canyon with an average width of 110 m. A topographic survey was performed with a total station survey instrument and several hundred points were collected to define the canyon topography and precise locations of approximately 50 different stage indicators. Deposits from the 1993 floods were easily identified by the lack of seasonal vegetation rooted in the sediment, unconformable relations to vegetation rooted in lower SWD, and an overall fresh appearance. SWD from 1993 overlay the all of the SWD described by O'Connor et al (1986), but were inset into and about 1.5 m below the top of the highest SWD that were identified during this survey of the reach. We observed that canyon expansion areas have the most extensive SWD; however, the sites with the thickest and highest deposits are small, protected alcoves along the margins of the flood flow

Types of High-water Marks Used in This Study

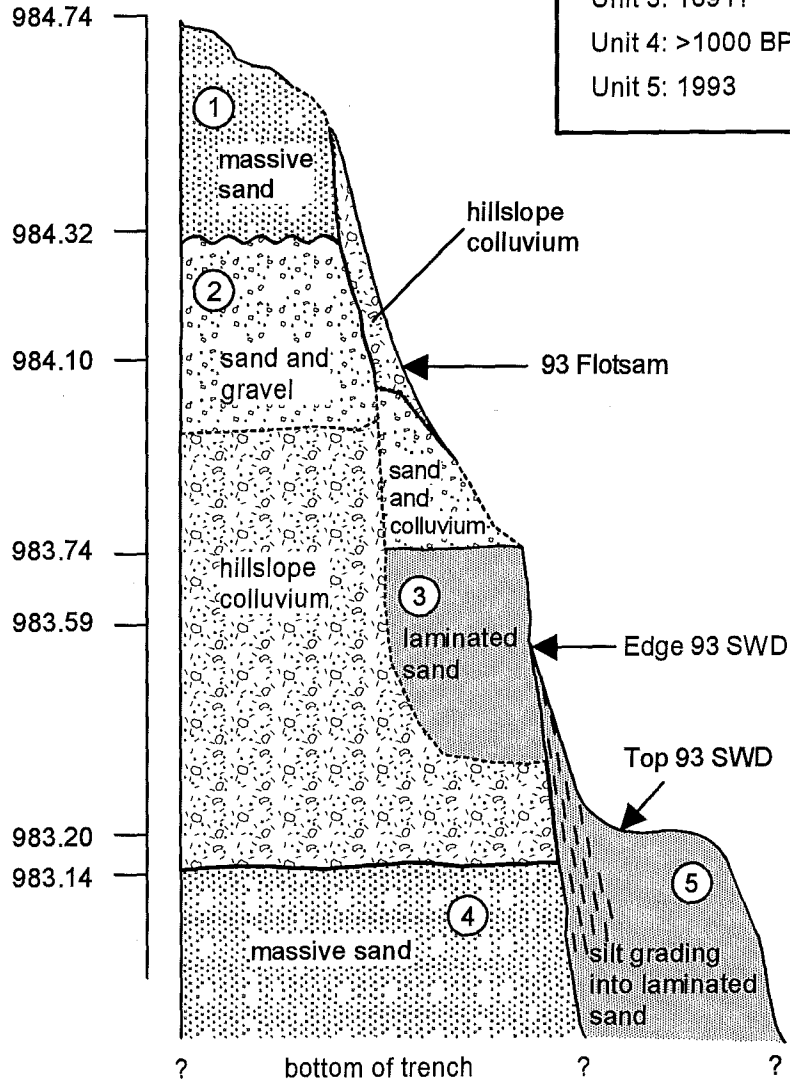
In the interest of developing a data set relating to most paleoflood studies we surveyed three types of flood stage indicators: flotsam, uppermost "edges" of slackwater deposits (ESWD), and the relatively flat "tops" of massive slackwater deposits (TSWD) (see figure 5, for example).

Flotsam includes any type of obviously floated delicate, organic material. In quiet-water areas along the margins of flow, flotsam deposits usually consisted of delicate organic material like small twigs and mats of leaves. At the very edge of inundation, flotsam was commonly deposited in fairly narrow, curvilinear arrangements conforming to the contours of the local topography. The 1993 flotsam along the perimeter of the reach was abundant, readily identifiable, and the highest points that we surveyed clearly represented the limit of inundation at that point. Delicate flotsam lines are the best indicators of the peak water surface, but their long-term preservation potential is poor.

We define the edge of a slackwater deposit (ESWD) as the uppermost elevation of the thin tapering "landward" edge of the deposit. During our survey, ESWD were often observed as thin drapes of fresh

Discharge Range from rating curve (n: 0.04-0.035)	Adjusted range
3843-4211	4996-5474 ^a
3441-3782	4473-4917 ^a
3240-3564	3240-3564 ^b
2916-3222	3791-4188 ^a
2787-3085	3240-3564 ^c
2500-2777	3240-3564 ^a
2433-2700	3163-3510 ^a

Elevation (m)



EXPLANATION
 Unit 1: ~ 1000 BP
 Unit 2: >1000 BP
 Unit 3: 1891?
 Unit 4: >1000 BP
 Unit 5: 1993

- a. 30% correction applied
- b. no correction applied--diagnostic indicator
- c. 16% correction applied for equivalence with flotsam estimate

Figure 5. Stratigraphic section and peak discharge estimates using a rating curve developed for section 7 of the Red Creek study reach. Discharge estimates in the left column are obtained directly from stage of the deposit and the associated discharge. Adjusted discharge estimates account for the underestimation of peak stage associated with slackwater deposits in this reach. No correction is applied to the 1993 flotsam-based discharge estimate.

sediment over hillslope colluvium or bedrock on the canyon margin. ESWD elevations were quite variable throughout the reach. Some tapered out at delicate flotsam lines, indicating deposition up to the water surface, but more often they were between the highest flotsam and the tops of the slackwater deposits. ESWD are important because they represent the highest level of sedimentation associated with a flood. However, their preservation potential is only poor to moderate because the layer of sediment is typically quite thin.

The tops of slackwater deposits (TSWD) are the most important and long-lived flood-related sedimentary features we observed. We define TSWD as the relatively flat surfaces on top of thick accumulations of slackwater sediment. An important distinction between TSWD and ESWD is the thickness of the underlying sediment. At each TSWD point it would have been possible to excavate and examine stratigraphy of the underlying deposit, whereas most of the ESWD points were just thin drapes of sediment (cm to mm). TSWD sites are much more likely to persist over long periods of time (100s to 1000s of years) than are the more ephemeral flotsam deposits and ESWD, and thus we conclude that they are representative of most SWD examined in paleoflood studies.

Hydraulic Modeling of the Red Creek Reach

In most paleoflood studies, flow modeling is typically a multi-stepped, trial and error procedure involving many variations in the initial water surface elevation, discharge, and channel roughness values. Each of these variables is either unknown or poorly constrained in a typical paleoflood study; however, in our study the initial condition of the starting water surface elevation was known due to the presence of many definitive HWMs, and our selection of appropriate n values was controlled by the constraints on the peak discharge previously described.

We contend that the February flood was most likely the largest to pass through the Red Creek reach during the winter of 1993, although the January peak was larger downstream at the TC gage; therefore, the peak discharge was probably between $3,370 \text{ m}^3 \text{ s}^{-1}$ and $3,512 \text{ m}^3 \text{ s}^{-1}$. In modeling the Red Creek reach, we found that the discharges associated with composite Manning's roughness coefficients (n) of 0.035 and 0.04 are $3,700 \text{ m}^3 \text{ s}^{-1}$ and $3,300 \text{ m}^3 \text{ s}^{-1}$ respectively, which effectively bracket the assumed "actual" peak discharge. The intermediate n -value of 0.0375 resulted in an estimate of $3,450 \text{ m}^3 \text{ s}^{-1}$ (figure 6), so this n -value is probably representative of the reach. The predicted water surface profile agrees well with the highest flotsam throughout the reach.

We visually fit water-surface profiles to the two other types of high-water indicators of interest in this study (ESWD and TSWD) in order to evaluate the discharge estimates associated with the highest points in each category (figure 6). In these modeling runs we altered the treatment of the initial conditions because of

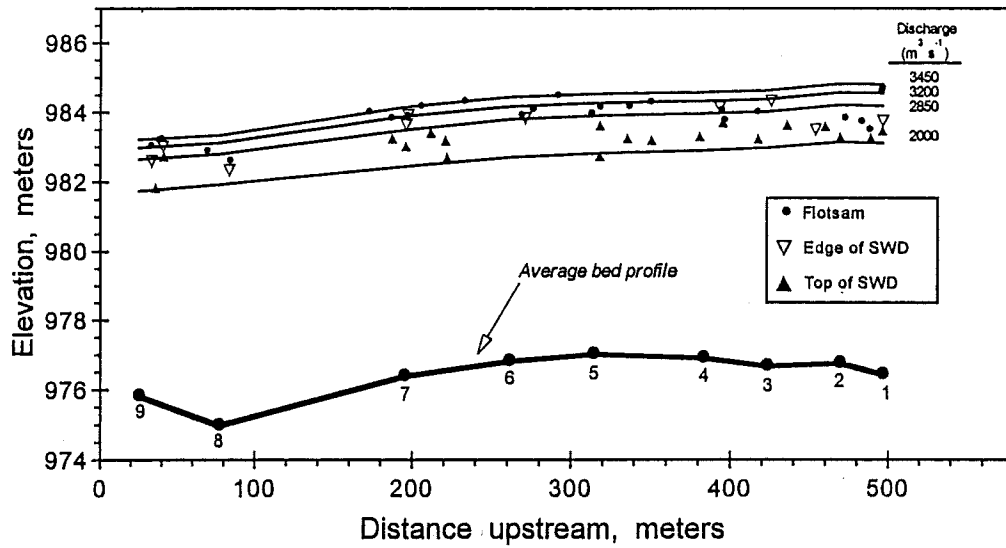


Figure 6. Example of the use of step-backwater modeling to visually estimate discharges associated with various types of water-surface indicators from the Red Creek reach. Profiles shown correspond to modeling with composite $n = 0.0375$. Cross section locations are numbered.

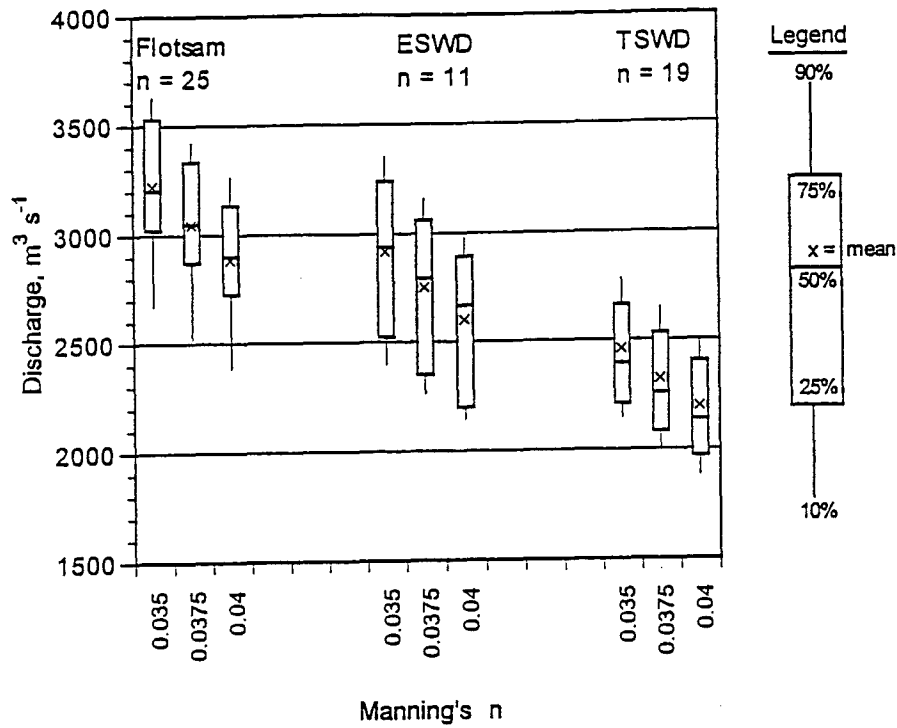


Figure 7. Box plot showing the discharge estimates associated with flotsam, edges of slackwater deposits, and tops of slackwater deposits. The effect of varying Manning's n values are also illustrated. Percentile boundaries of data sets shown in legend.

	Flotsam			ESWD			TSWD		
	0.035	0.0375	0.04	0.035	0.0375	0.04	0.035	0.0375	0.04
Mean	3211	3035	2873	2908	2741	2590	2450	2311	2185
Std. Dev.	350	335	322	374	359	343	270	258	245
Max.	3669	3444	3282	3370	3178	3024	3029	2823	2647
Min.	2425	2270	2136	2378	2254	2143	1995	1887	1788

Table 3. Comparison of discharge estimates for various types of stage indicators using a range of Manning's n values.

greater uncertainty in the appropriate starting water-surface elevation. The HEC-2 program has an option to calculate the initial water-surface elevation using a slope-area calculation. In this procedure, the user provides an estimated starting elevation, a “known” discharge, and a “known” energy gradient. The program first calculates a water surface elevation that balances with the “known” parameters through an iterative procedure. Once the balance is obtained, the computations proceed through the reach. We used the water surface slope measured from flotsam at the downstream end of the reach to represent the energy gradient in our attempts to model profiles consistent with the ESWD and TSWD points. In these additional modeling scenarios, we retained the composite n value range of 0.035-0.04.

Point-Rating Estimates of Discharge

Most previous SWD-PSI paleoflood studies have relied on bracketing SWD and PSI between successive water-surface profiles to estimate a range of associated peak discharges; thus the basis for the reported discharge or range of discharges is visual (O'Connor and Webb, 1988). This technique is generally adequate given the variety of uncertainties in indirect discharge estimation of large flood discharges; however, it does not necessarily provide detailed information about the actual spread of discharges associated with individual stage indicators, which is a principal goal of our study. In addressing this, we adopted a method that assigns specific discharge values to each individual stage indicator in the reach. This approach, which we have termed the “point-rating” method involves a more rigorous evaluation of model output and allows for a more precise evaluation of the spread of the associated discharge estimates, a more direct comparison of estimates from flotsam and slackwater deposits, and a better evaluation of stage indicators located between cross sections.

Placement of the SWD and PSI along the longitudinal profile of the channel in the correct position for comparison to the estimated water-surface profiles can be a subjective and potentially arbitrary procedure, particularly on large streams. In developing the point-ratings we adopted a set of simple, linear equations to make this and the determination of discharge more accurate and systematic. First, the mid-channel profile was divided into straight subreaches and the stage indicators within each sub-reach were then projected along a line perpendicular to the mid channel line. The elevation and distance from the downstream end of the reach were used to precisely locate each point in its proper position along the profile. A set of simple linear equations was used to determine the elevation corresponding to each point's longitudinal position on bracketing water-surface profiles separated by $200 \text{ m}^3 \text{ s}^{-1}$ increments, and another linear relation determined the discharge at the point's vertical position by defining the stage-discharge relation at its longitudinal position. This method was applied to the results of modeling scenarios using n values of 0.035, 0.0375, and 0.04. The results are summarized in table 3 and figure 7.

The relative distribution of the point-rating discharge estimates are generally consistent with the visual discharge estimates. The highest flotsam corresponds to the highest discharges, TSWD to the lowest discharges, and ESWD to intermediate values. The variability in the estimates from each type of indicator reflects uncertainties faced in any attempt to indirectly estimate the peak discharges of large floods because of the complex, multi-dimensional nature of flooding. Flotsam was identified at various levels in the reach, suggesting that relatively steady conditions may have prevailed at various times during the waning of the floods and/or the flotsam deposits may have been emplaced randomly as the flood stage decreased. Variability of the SWD elevations may reflect a similar waning-stage phenomenon, but deposition could occur simultaneously at different levels in different settings depending on local geometric constraints (Kochel and Baker, 1988). These factors reinforce the importance of focusing on the trends of the highest indicators of each category when estimating peak discharges.

The most conservative peak discharge estimates are those associated with the highest elevations from each indicator category. The following ranges correspond to composite n values of 0.04 and 0.035, respectively. The range of the maximum flotsam estimate is 3282-3670 $\text{m}^3 \text{s}^{-1}$; the range of the maximum ESWD estimate is 3024-3370 $\text{m}^3 \text{s}^{-1}$; and the maximum TSWD estimate is 2647-3029 $\text{m}^3 \text{s}^{-1}$. If a typical paleoflood study were conducted at the Red Creek site several decades hence, researchers would likely establish a peak discharge estimate corresponding to the maximum TSWD estimate obtained in our study. This would, of course, constitute a minimum estimate. The SWD-based underestimation expressed in this data set ranges from 22% to as much as 49%, based on comparing the maximum FLT estimate to the maximum and average TSWD estimates, respectively. The percentage differences between the variety of indicators is outlined in table 4.

We believe that bracketing the HWMs between successive profiles or simply enveloping the highest indicators with an individual profile are reasonable techniques for discharge estimation in the context of paleofloods, historical floods, and recent large floods given the variety of potential uncertainties in each case. The point rating technique is illustrated here simply as a convenient means of precisely determining the limits of the bracketing discharges and, in this sense, is superior to specifying a discharge range simply from the basis of a visual assessment.

Cross-Section Rating Discharge Estimates

The development of a rating curve at an individual cross section following the formulation of a successful modeling scenario of an entire reach is another method for discharge estimation commonly employed in paleoflood studies. Rating curves are useful at sites where a stratigraphic exposure of paleoflood deposits is located. In our study, cross-section 7 contains both the variety of 1993 high-water

		Peak discharge estimates ($\text{m}^3 \text{s}^{-1}$)			
		Point-Rating Analysis			Rating Curve
Indicator Type		Min	Mean	Max	Max
TSWD		1887	2311	2823	2646
ESWD		2254	2741	3178	2939
FLT		2270	3035	3444	3400
		Percentage difference between discharge estimates			
		<i>(relative to max. flotsam estimate)</i>			
FLT and TSWD		82.5	49.0	22.0	28.5
FLT and ESWD		52.8	25.6	8.4	15.7

Table 4. Comparison of the differences between discharge estimates based on SWD and flotsam using the point-rating method and a rating curve for one section.

marks and an exposure of SWD stratigraphy that records at least 4 large floods prior to 1993 (figure 5). The highest slackwater deposits identified at this site are approximately 1.5 m higher than the highest deposits identified by O'Connor et al (1986). The capping deposit is probably correlative with the 1000 year BP paleoflood described at the Ely-Baker reach (Ely and Baker, 1985).

The discharges associated with the different types of indicators in section 7 from the 1993 flooding are as follows, assuming n values of 0.035 and 0.04: flotsam, 3240-3564; ESWD, 2737-3085; and TSWD, 2500-2777. Using the average values from each range, the measures of SWD-based underestimation are 18% (flotsam and ESWD) and 30% (flotsam and TSWD). These results are consistent with the estimates based on the point-rating of the entire reach. The maximum difference in the peak discharge estimated from flotsam in the point-rating method and the section rating method is only 3%. Differences in the maximum discharge estimates reflect variability inherent to the nature of the data.

Section Rating Estimates from the Ely-Baker Reach

We observed that SWD and flotsam can have considerably less vertical separation in areas where the confining slope is less steep. At a site in the Ely-Baker reach downstream, we assessed the SWD-based underestimation in addition to the flotsam-based peak discharge estimate described previously. At this site there was a relatively small difference between the elevations of the highest flotsam and TSWD (~30 cm). The discharge corresponding to the flotsam was $3680 \text{ m}^3 \text{ s}^{-1}$ ($130,000 \text{ ft}^3 \text{ s}^{-1}$), and the discharge corresponding to the TSWD was $3500 \text{ m}^3 \text{ s}^{-1}$ ($123,600 \text{ ft}^3 \text{ s}^{-1}$). The associated SWD underestimation factor is thus only about 5%. We hypothesize that the smaller difference in flotsam and TSWD-based discharge estimates is controlled by the geometry of the depositional site, which is a broad embayment at the mouth of a small tributary. The more gradual slope of this site and the greater width of the river were apparently conducive to sedimentation up to level very near the peak water surface in the sense that the “top” and “edge” of the deposit were essentially the same thing. This small difference may explain in part why the modeling results reported by Ely and Baker (1985) from this reach were consistent with the TC gage estimates. Their discharge estimate for the 1980 flood was within 1% of the gage estimate, and their estimate for the 1951 flood was within 15% of the gage estimate. The 1980 estimate was based on flotsam, whereas the 1951 estimate was based on SWD.

Evaluation of Results

The whole-reach (point-rating) and single-site rating approaches produced maximum peak discharge estimates that differ by only 3%. Estimates of SWD-based underestimation are also similar. Based on the point-rating data, the underestimation factor ranges from 22-49% (based on difference in maximum and average values respectively); and using the single-section rating curve the factor was 30%. Given that the

highest indicator in a given category would be sought in a paleoflood study at this site, we believe that 30% is a reasonable, conservative measure. The amount of underestimation is controlled in part by the general geometry of the depositional environments typical of this reach and probably varies as a function of flood stage. The 5% underestimation factor from the Ely-Baker reach illustrates the effect of depositional environment. In general the highest slackwater deposits on the Red Creek reach are in small, protected alcoves along the channel margins. At these sites, the edges of the depositional areas are confined by steep canyon walls which apparently constrained the vertical limit of sedimentation to an average depth of about 1 m below the water surface. The site we investigated in the Ely-Baker reach was a gently sloping bench of sediment in a tributary embayment, and the cross-section was wider than any in the Red Creek reach. Here, the difference in elevation between SWD and flotsam was only 30 cm.

Discussion - Reconciliation of Discharge Estimates for Verde River Floods

The original study at the Red Creek reach by O'Connor and others (1986) was performed as an independent test of the reproducibility of the results described by Ely and Baker (1985). They concluded that their results confirmed the flood chronology and relative flood magnitudes reported by Ely and Baker (1985), but their discharge estimates for assumed correlative flood deposits were considerably lower and the 1,000 year BP flood deposit was not identified. O'Connor and others (1986) concluded that much of the discrepancy was from differences in drainage area and the fidelity of the SWD elevations to the peak water surface at each site. Our restudy of the Red Creek reach confirms the importance of these factors by documenting the magnitude of their influence on peak discharge estimates. In addition, we found evidence for what we believe is the 1,000 year BP flood, and we have an alternative interpretation of the deposits likely associated with historical floods that is more consistent with the Ely-Baker reach and the gage. Each of these factors, SWD-based underestimation, contributing drainage area differences, and new stratigraphic evidence, is critical in reconciling the differences between the discharge estimates from the two paleoflood study sites and the TC gage.

SWD-based Underestimation

The effect of SWD-based underestimation is an obvious control on large differences in paleoflood estimates from disparate sites. This phenomenon is particularly critical in comparisons of SWD-based estimates to similar estimates from diverse settings and to gaged estimates. Discharge estimates for flood peaks in excess of $1,000 \text{ m}^3 \text{ s}^{-1}$ on the Verde River from paleoflood studies and gaging stations are depicted in figure 8 (see also tables 5 and 6). Estimates from the Red Creek reach and the Ely-Baker reach are shown as ranges. The lower end of the range corresponds to the maximum reported, SWD-based estimates for the given flood or series of floods. The upper limit corresponds to that value adjusted by the

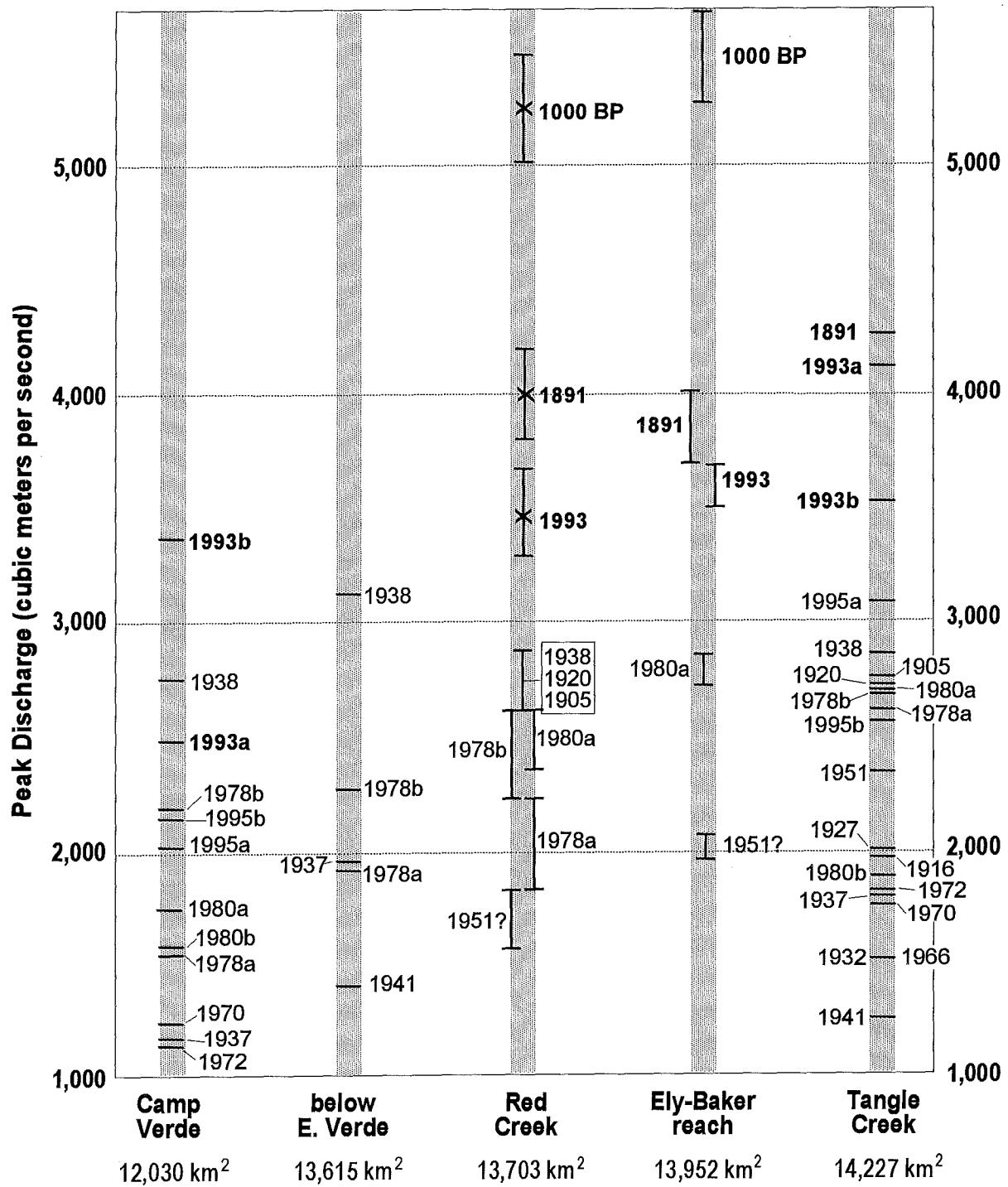


Figure 8. Summary diagram of gaged, historical, and paleoflood peak discharge estimates for the lower Verde River. Total drainage area to each site is shown. The gage record is longest for Tangle Creek and its predecessors; the Camp Verde record begins in 1936, and only a few large floods were recorded at the now defunct gage near the E. Verde River confluence. Paleoflood estimates from the Red Creek and Ely-Baker reaches are shown as ranges, with a x marking the preferred estimate. They are based on our 1993 field studies and upward adjustment of previous paleoflood discharge estimates from Ely and Baker (1985) and O'Connor et al (1986), based on our recent work.

Comparison of discharges from sites along the lower Verde River: gaging stations

Year	Month	Day	Near Camp Verde (09506000)		Below East Verde (09508000)		Below Tangle Ck. (09508500)	
				<i>note</i>		<i>note</i>		<i>note</i>
1995	3	6	2,138	<i>a</i>	-		2,543	<i>a</i>
1995	2	15	2,022	<i>a</i>	-		3,059	<i>a</i>
1993	2	20	3,370	<i>h</i>	-		3,512	<i>h</i>
1993	1	8	2,478	<i>h,i</i>	-		4,106	<i>h</i>
1980	2	20	1,589	<i>b,c</i>	-		1,863	<i>c</i>
1980	2	15	1,753	<i>b,c</i>	-		2,685	<i>e</i>
1978	12	19	2,192	<i>b,c</i>	2,249	<i>g</i>	2,662	<i>e</i>
1978	3	1	1,552	<i>b,c</i>	1,914	<i>f</i>	2,588	<i>e</i>
1972	10	20	1,150	<i>b,c</i>	-		1,795	<i>e</i>
1970	9	5-6	1,247	<i>b,b</i>	-		1,753	<i>e</i>
1966	12	7	-		-		1,501	<i>e</i>
1951	12	31	-		-		2,311	<i>d,e</i>
1941	3	14	850	<i>e</i>	1,408	<i>d</i>	1,240	<i>d,e</i>
1938	3	3-4	2,747	<i>e</i>	3,115	<i>d</i>	2,832	<i>d,e</i>
1937	2	7	1,181	<i>d,e</i>	1,943	<i>d</i>	1,784	<i>d,e</i>
1932	2	9	-		-		1,501	<i>d,e</i>
1927	2	17	-		-		1,982	<i>d,e</i>
1920	2	22	-		-		2,690	<i>e</i>
1916	1	20	-		-		1,951	<i>d,e</i>
1905	11	27	-		-		2,719	<i>d,e</i>
1891	2	24	-		-		4,248	<i>d,e</i>

Notes

- a. provisional data provided by USGS
- b. discharge recorded at gage #09505550, "below Camp Verde", value in table includes peak from West Clear Creek (station 09505800) for comparison to values from station 09506000
- c. Chin, Aldridge, and Longfield, 1991
- d. Patterson and Somers, 1966
- e. Garrett and Gellenbeck, 1991
- f. Aldridge and Eychaner, 1984
- g. Aldridge and Hales, 1984
- h. USGS, Water Resources Data, Arizona, Water Year 1993
- i. only 57% of peak contributed to peak at Tangle Creek gage

Table 5. Summary of discharge estimates for large historical floods at gaged sites on the lower Verde River. See Patterson and Somers (1966) for gage histories.

Comparison of discharges from sites along the lower Verde River: paleoflood study sites

Date	Red Creek Reach					Ely-Baker Reach				
	Reported		Adjusted (30%)		notes	Reported		Adjusted (5%)		notes
	min	max	min	max		min	max	min	max	
1993	-	-	3282	3664	<i>a</i>	-	-	3500	3680	<i>e</i>
1980	1800	2000	2340	2600	<i>b</i>	-	2700	2700	2835	<i>d</i>
1978b	1700	2000	2210	2600	<i>b</i>	-	-	-	-	
1978a	1400	1700	1820	2210	<i>b</i>	-	-	-	-	
1951	1200	1400	1560	1820	<i>b</i>	-	1950	1950	2048	<i>d</i>
1938	2000	2200	2600	2860	<i>b,c</i>	-	-	-	-	
1920	2000	2200	2600	2860	<i>b,c</i>	-	-	-	-	
1905	2000	2200	2600	2860	<i>b,c</i>	-	-	-	-	
1891	2916	3222	3791	4188	<i>c,f,g</i>	3500	3800	3675	3990	<i>f</i>
1000 BP	3843	4211	4995	5474	<i>c,f,g</i>	5000	5400	5250	5670	<i>f</i>

Notes

- a. range from this study associated with highest flotsam and range of Manning's n: 0.035 - 0.04
- b. reported ranges based on examination of water-surface profile and SWD comparisons in O'Connor et al. (1986)
- c. value corresponds to identification and/or reinterpretation of SWD stratigraphy from this study
- d. reported range corresponds to single value reported in Ely and Baker (1985) and equivalent adjusted values
- e. range corresponds to discharge estimate from TSWD and Flotsam
- f. range corresponds to TSWD estimate and adjusted equivalent
- g. range corresponds to TSWD estimates from rating curve (n: 0.035 - 0.04) and equivalent adjusted values

Table 6. Comparison of paleoflood discharge estimates from the Red Creek and Ely-Baker reaches on the Verde River. Reported values are from the original studies; adjusted values reflect corrections for SWD-based underestimation determined in this study.

underestimation factors derived in our study (table 6). Clearly, accounting for underestimation has a significant effect on the comparison and reduces the apparent discrepancy considerably.

Contributing Drainage Area

Consideration of the influence of drainage area provides further reinforcement for the consistency of the record throughout the basin. Peak discharges for virtually every flood in the gage record increase with increasing drainage area in the lower Verde basin. The only exception is the 1938 flood discharge. The 1993 floods provided very dramatic examples of the variable influence of increasing drainage area on peak discharges. In the January 1993 flood the discharge nearly tripled between CV and TC, while the February 1993 flood underwent a negligible increase. As shown in figure 8, the January event is the most extreme example of discharge increasing downstream in the systematic record. Several other floods behaved like the February 1993 flood, but most floods showed gradual increases in peak discharge with increasing drainage area. Relatively minor differences in contributing drainage area can have a large effect on peak discharge estimates from sites that are relatively close together if these sites happen to be along a reach that received substantial tributary input.

Paleoflood Stratigraphy

Our identification and interpretation of the SWD sequence in section 7 of the Red Creek reach offers a final element to the reconciliation of the discharge estimates from the various sites. It also extends the paleoflood record preserved in the Red Creek reach and helps to clarify uncertainty concerning the 1938 and 1891 floods as interpreted in the previous paleoflood study at the Red Creek site.

The newly discovered stratigraphic exposure at cross section 7 of the Red Creek reach reveals evidence for at least two paleofloods larger than the 1993 event that are probably 1,000 years old or more (see figure 5). We tentatively correlate the highest deposit with the uppermost deposit of the Ely-Baker reach, whose age has been constrained to 1,000 years BP by a ^{14}C date of in situ charcoal and diagnostic Hohokam artifacts found on the surface of the deposit (Ely and Baker, 1985). The correlation is based on relative topographic positions of the deposits and the discharge estimates associated with them. We identified similarly high and probably correlative flood deposits at four other sites in the Red Creek reach. The discharge at section 7 that corresponds to the highest deposits is $5000\text{-}5474\text{ m}^3\text{ s}^{-1}$ (176,700-193,300 cfs). The maximum adjusted point-rating estimate from a likely correlative, but slightly higher deposit at another site in the reach is $5405\text{-}6200\text{ m}^3\text{ s}^{-1}$ (190,875-219,000 cfs). The adjusted estimate from the Ely-Baker reach is $5940\text{ m}^3\text{ s}^{-1}$ (210,000 cfs). The underlying flood deposits (units 2 and 4) obviously predate unit 1, but the lack of any direct numerical control on these units precludes any specific age estimate for the associated floods.

The flood deposit that is inset below these deposits but above the highest 1993 flood deposit (unit 3 in figure 5) may have been emplaced by the 1891 flood. The peak discharge of this flood above the confluence of the Verde and Salt rivers was estimated as about $4,200 \text{ m}^3 \text{ s}^{-1}$ (150,000 cfs; Patterson and Somers, 1966). Ely and Baker (1985) identified a likely 1891 SWD in their reach that corresponds to an adjusted discharge estimate of $4180 \text{ m}^3 \text{ s}^{-1}$ (147,600 cfs). In the Red Creek reach, O'Connor et al (1986) interpreted a considerably lower SWD as corresponding to the 1891 flood. The adjusted discharge estimate for this SWD is approximately $3100 \text{ m}^3 \text{ s}^{-1}$ (109,500 cfs). This difference implies a larger increase between the Red Creek and Ely-Baker sites than the January 1993 flood. This is possible; but, we think that it is more likely that this deposit is from the 1938 flood. This event had peak discharges of $3100 \text{ m}^3 \text{ s}^{-1}$ at the gage below the Verde - East Verde river confluence (figure 2) and $2800 \text{ m}^3 \text{ s}^{-1}$ at a site about 10 km downstream from the present TC gage. Assuming that these gaged peaks are reasonably accurate, then at the Red Creek site the peak discharge would have been in the range of the 1891 flood discharge estimated by O'Connor and others (1986). The 1938 flood deposits were probably buried by the 1993 floods. If this scenario is correct, then the adjusted discharge estimates for the 1891 flood at the Red Creek and Ely-Baker reaches are $3790\text{-}4200 \text{ m}^3 \text{ s}^{-1}$ (133,900-148,300 cfs) and $4180 \text{ m}^3 \text{ s}^{-1}$ (147,600 cfs), respectively.

The scenario outlined above reconciles the gaged, historical, and paleoflood data quite well, but in the absence of better numerical age constraints on the various flood deposits it remains somewhat speculative. If the high inset deposit shown in figure 5 is not an 1891 flood deposit, then the 1891 flood at Red Creek was evidently smaller than the 1993 flood and the associated SWD are buried. In this less likely scenario, the high inset deposit represents a flood that occurred sometime between 1,000 years BP and 1891, and the location of the 1938 deposit is unresolved.

Stratigraphic Implications of the Complex Flood Record

The potentially large influence of drainage area on peak discharge in a small portion of the Verde River basin reveals potential complexities in the hydrology of extreme floods on the Verde River (i.e. those involving large runoff contributions from much of the basin). The corresponding stratigraphic record of flooding at disparate sites would reflect this. Our approach to reconciliation was useful in interpreting the largest floods at each site but it relied heavily on gage data. Detailed correlation of a more complete paleoflood chronology incorporating higher frequency events from several sites would be a daunting challenge.

A complicating factor results from the fact that variations in the relative contribution of runoff from the middle and lower parts of the Verde basin in different floods caused the relative magnitude of some floods to be inverted between CV and TC and sites between them. In fact, we believe that the cross-over point was

between the Red Creek and Ely-Baker reaches in the 1993 floods. The recent flood history of the lower Verde River has two additional examples of this phenomenon occurring in years in which two large flood peaks occurred (1980, 1993, 1995). As illustrated in figure 8, the relative ranking of large gaged floods at CV, in order of decreasing size, is Feb. 1993, 1938, Jan. 1993, Dec. 1978, Mar. 1995, Feb. 1995, 1980, and Mar. 1978. At TC the relative ranking is Jan. 1993, Feb. 1993, Feb. 1995, 1938, 1980, Dec. 1978, Mar 1978, and Mar. 1995. Note that the differences between peak discharges for all of the gaged floods except the Jan. 1993 and the Feb. 1995 floods decreased substantially between CV and TC, so that many floods cluster in the $2,500$ to $2,800 \text{ m}^3 \text{ s}^{-1}$ (90,000 to 100,000 cfs) range. This implies that attempts to correlate depositional stratigraphy from floods with peak discharges less than about $2800 \text{ m}^3 \text{ s}^{-1}$ (100,000 cfs) on the lower Verde River would be very complicated.

To illustrate this, figure 9 shows two schematic, idealized stratigraphic columns that correspond to the flood records from CV and TC. This depiction assumes ideal conditions of deposition and preservation and is purely for illustrative purposes. Nonetheless, it reveals the level of complexity that may be encountered in attempting to unravel the historical record of flooding on the lower Verde River as recorded in the flood stratigraphy, particularly for events less than about $2800 \text{ m}^3 \text{ s}^{-1}$. This illustration underscores the potential difficulties in correlating floods from various, disparate paleoflood sites on a river without the aid of a reasonably detailed historical record and an adequate understanding of the flood hydrology of the basin.

Flood-Frequency Analysis

We used the results of our assessment of the potential underestimation of peak discharges based on SWD to conduct a revised flood-frequency analysis of the Verde River. A previous analysis by Stedinger and others (1986) using the MAX program incorporated paleoflood, historical, and systematic discharge estimates for the Verde River. The MAX program uses maximum likelihood estimators in the statistical analysis of both the systematic (gaged) and categorical (paleoflood) data. Categorical data is defined by the number of occurrences or non-occurrences above specific magnitude thresholds over specified amounts of time and is compatible with the nature of the paleoflood data. This statistical approach has proven to be superior in extracting information from compound data sets as compared to the weighted moments technique recommended by the United States Water Resources Council Bulletin 17b (1982) (Stedinger and Baker, 1987; Lane, 1987, Condie and Lee, 1982). The statistical details of this approach and its application to paleoflood data are provided by Stedinger and Cohn (1986), and Stedinger and others (1986). In their original analysis, the use of paleoflood data produced a somewhat lower 100-year discharge estimate than the historical and gage data only. In our revised analysis, we updated the

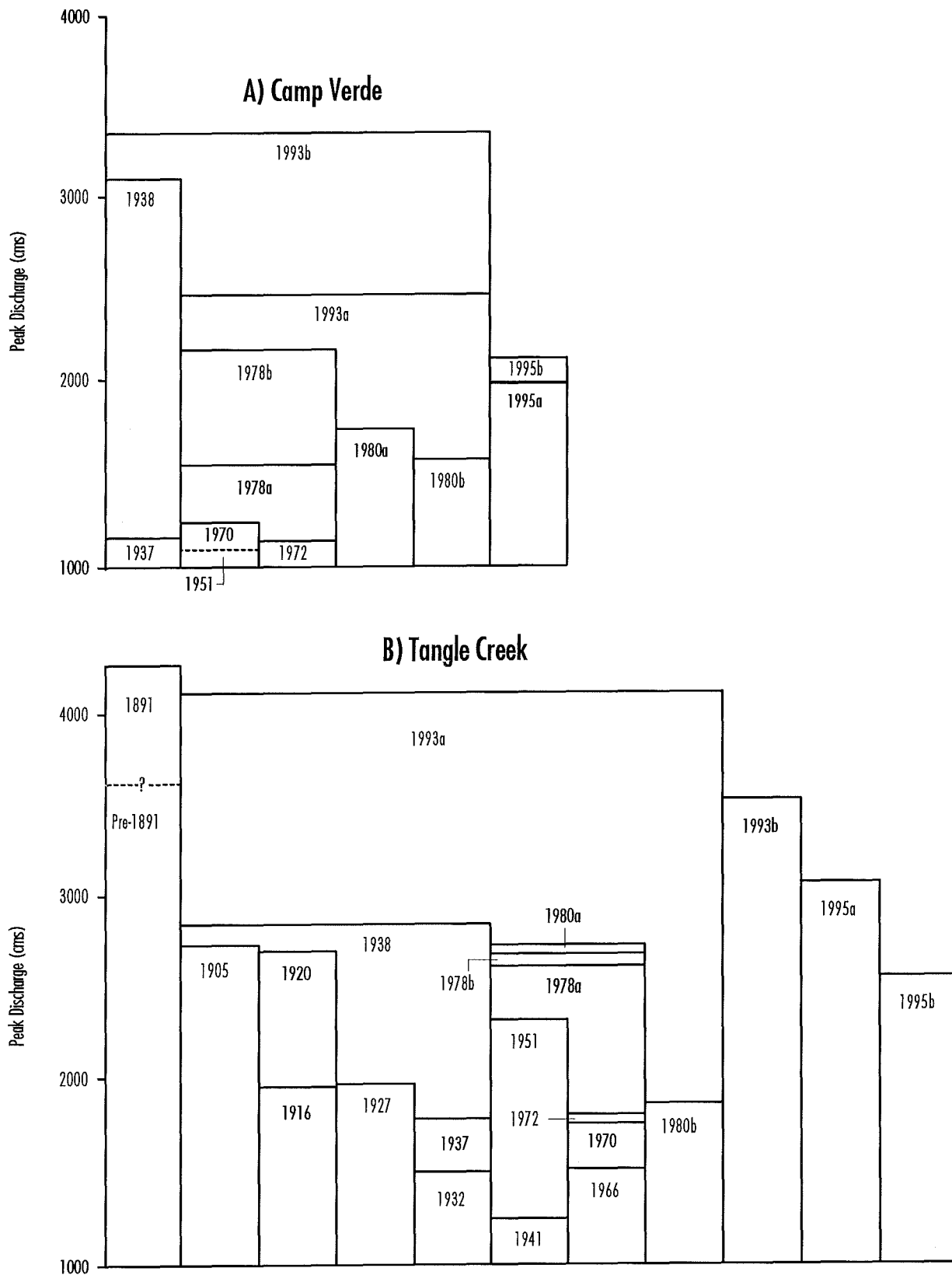


Figure 9. Hypothetical flood-deposit stratigraphy from historical floods at sites near the Camp Verde and Tangle Creek gages on the Verde River. These stratigraphic sequences assume that deposits from all floods with peak discharges of greater than 1000 cms are preserved, and deposition occurred up to the peak water surface. Deposits from smaller floods are inset into existing deposits, whereas larger floods overtop existing deposits. Discharges are listed in table 5.

systematic record through 1995, adjusted the paleoflood discharges upwards, and shortened the inferred length of the geologic record of flooding.

In a previous paleoflood study on the Verde River, generalizations about the potential longevity of flood scars and scour marks on canyon walls were used to extend the length of the paleoflood record to 2000 years (Ely and Baker, 1985). The geological arguments for these inferred record length are reasonable but not very quantitative or well-constrained. In this analysis, we constrain the length of the flood record to the estimated age of the oldest dated flood deposit on the lower Verde River (1000 BP). Also, because of the influence of contributing area on the flood magnitudes along the Verde River, we concluded that paleoflood data from the Red Creek reach cannot be reliably integrated with the gage data from TC. Furthermore, our observations of the different amount of SWD-based underestimation at each site indicate that use of a 5% factor in adjusting discharges from the Ely reach is appropriate.

In the flood-frequency analysis, we modeled two scenarios: (1) simply updating the original analysis from Stedinger and others (1986) through 1995 to reflect the measurement of large floods at the gage in 1993 and 1995 (peaks of 4106 and 3058 m³ s⁻¹, respectively), but making no other changes; (2) including the updated historical record, shortening the total record length to coincide with the oldest dated paleoflood event (1000 years), adjusting the SWD-based discharge estimates from the Ely reach by 5% and treating the 1000 BP discharge estimate as a minimum constraint with no upper bound. We prefer scenario 2 because it incorporates more well-constrained paleoflood information and is probably a more realistic treatment of the data.

The predicted 100-year flood from scenario 1 is essentially the same as the value reported by Stedinger and others (1986) in the original analysis (table 7). This is somewhat surprising considering the addition of two large floods, one of which (1993) is the flood of record. In scenario 2, the predicted 100-year flood increased by 28% relative to the scenario 1 prediction. Clearly, the addition of the two recent peaks combined with the modifications of the paleoflood data have a significant effect on the results. Our revised 100-year flood estimate is comparable to estimates from various conventional statistical analyses of the systematic and historical data (table 7); however, no statistical analysis of the historical and systematic data listed in the table includes the most recent large floods.

Estimates of the magnitude of lower frequency events from our analysis as well as a variety of other methods listed in table 7 stand in stark contrast to estimates of the probable maximum flood (PMF) on the Verde River attributed to the U.S. Army Corps of Engineers and the U.S. Bureau of Reclamation (reported in Ely and others, 1988). There is no geological evidence of such extreme flooding on the Verde River, and we believe that it is reasonable to conclude that no floods approaching the reported PMF magnitudes have

Maximum Discharges			
Paleoflood Studies (as reported)			
<i>Ely and Baker (1985)</i>	5,400		
<i>O'Connor et al. (1986)</i>	2,400		
<i>This study</i> ¹	5,474		
Discharge-Drainage Area Relations			
<i>Malvick (1980)</i>	5,950		
<i>Enzel et al. (1993)</i> ²	6,500		
Probable Maximum Flood			
<i>U.S. Army Corps of Engineers</i> ³	18,970		
<i>U.S. Bureau of Reclamation</i> ³	21,640		
Statistical Analysis			
Systematic and historical data	100-yr	500-yr	1000-yr
<i>Anderson and White (1979)</i>	4,500	-	-
<i>Roeske (1978)</i>	4,000	6,550	-
<i>Garrett and Gellenbeck (1989)</i>	4,640	-	-
Geological, historical, and systematic data			
<i>Stedinger et al.</i>			
<i>original</i>	3,115	-	4,220
<i>updated (scenario 1, this study)</i>	3,144	4,083	4,475
<i>This study (scenario 2)</i>	4,021	5,350	5,936
<i>notes</i>			
1. from section 7 rating curve			
2. visual estimate from envelope curve			
3. as reported in Ely et al. 1988			

Table 7. Comparison of various theoretical and empirical estimates of discharge for the lower Verde River.

occurred on the Verde River during at least the last 10,000 years (i.e. the Holocene). If such extraordinary floods had occurred in this time we would expect to find at least some compelling geomorphic evidence attesting to that fact.

Conclusions

Our analysis of the 1993 floods on the Verde River illustrate that important advancements in understanding the flood hydrology of a given drainage basin can result from integrating paleoflood data with available gage and historical flood data. Our study also illustrates the potential magnitude of some important uncertainties faced in most paleoflood reconstruction attempts. We found reasonably consistent relationships between the elevations of slackwater deposits and ephemeral indicators of the actual peak flood stage. In steep-walled depositional settings on the Verde River, slackwater deposits were about 1 m below the peak water surface. Using these elevation differences in step-backwater modeling, we estimate that discharge estimates based on slackwater deposits are about 30% less than the actual peak discharge. In settings where confining slopes are more gentle, differences in these discharge estimates are less than 10%. Using these relationships, we revised upward previously reported paleoflood estimates for the Verde River. Corrections for discharge underestimation from reliance on SWD, recognition of the potentially great importance of differences in contributing drainage area, and identification of undocumented SWD stratigraphy contribute to a consistent relationship between discharges estimated at the two paleoflood reaches and the upstream and downstream gages. This study conclusively demonstrates the importance of understanding the flood hydrology of a river basin when interpreting paleoflood evidence in the basin.

Incorporation of our study results into previous paleoflood-based flood frequency analyses result in higher predicted magnitudes for low-frequency events than previously reported. The new estimate of the so-called 100-year flood is comparable to that most recently reported by the USGS (Garrett and Gellenbeck, 1991); however, their analysis does not include the 1993 or 1995 floods. All of the statistical and empirical predictions of low-frequency flood magnitudes listed in table 7 support the conclusion that assessments of the PMF for the Verde River Basin is unrealistically large. Our field studies confirm that there is no evidence of floods having such high magnitudes in the Holocene record of flooding.

Integrating our 1993 and revised paleoflood estimates with the gage data for the Verde River reveals much about the complexity of flooding on this river system. The two large floods of 1993 behaved quite differently and thereby increased our ability to understand the genesis of large floods on the Verde River. This information can be related to gaged, historical, and paleoflood records alike. Many large floods of the gaged record, including the February 1993 flood, emanated almost entirely from the upper Verde basin above CV. In the January 1993 flood, more than 65% of the peak discharge came from the lower 25% of

the Verde basin. This situation caused a rapid, dramatic increase in the peak discharge downstream of CV. As a consequence, sites only a few kilometers distant from one another along the lower Verde had substantially different peak discharges. Similar but less extreme scenarios are evident in the systematic record and very likely in the paleoflood record, a point with important implications for differences in paleoflood stratigraphy at different sites along the river. The combined hydroclimatological and hydrological characteristics that distinguished the floods of January and February 1993 establish a general framework that easily substantiates the stratigraphic evidence for the occurrence of floods considerably larger than the 1993 events.

References

- Aldridge, B.N., and Eychaner, J.H., 1984, Floods of October 1977 in southern Arizona and March 1978 in central Arizona: U.S. Geological Survey Water-Supply Paper 2223, 143 pp.
- Aldridge, B.N., and Hales, T.A., 1984, Floods of November 1978 to March 1979 in Arizona and west-central New Mexico: U.S. Geological Survey Water-Supply Paper 2241, 149 pp.
- Anderson, T.W., and White, N.D., 1979, Statistical summaries of Arizona streamflow data: U.S. Geological Survey Water-Resources Investigation 79-5, 416 pp.
- Baker, V.R., 1989, Magnitude and frequency of paleofloods: *in* Floods: Hydrological, Sedimentological, and Geomorphological Implications, edited by K. Beven, and P. Carling, John Wiley, New York, pp. 171-183.
- Baker, V.R., 1987, Paleoflood hydrology and extraordinary flood events: *Journal of Hydrology*, v. 96, p. 79-99.
- Baker, V.R., and Kochel, R.C., 1988, Flood sedimentation in bedrock fluvial systems: *in* Baker, V.R., Kochel, R.C., and Patton, P.C., Flood Geomorphology: New York, Wiley, pp. 123-138.
- Benson, M.A., and Dalrymple, T., 1967, General field and office procedures for indirect discharge measurements: USGS Techniques of Water Resource Investigations, Book 3, chapter A-1, 30 pp.
- Chin, E.H., Aldridge, B.N., and Longfield, R.J., 1991, Floods of February 1980 in southern California and central Arizona: U.S. Geological Survey Professional Paper 1494, 126 pp.
- Condie, R. and Lee, K., 1982, Flood frequency analysis with historic information: *Journal of Hydrology*, vol. 58, pp. 47-61.
- Dalrymple, T., and M.A. Benson, 1967, Measurement of peak discharge by the slope-area method: U.S. Geol. Surv. Techniques of Water Resource Investigations, Book 3, chapter A-2, 12 pp.
- Ely, L.L., 1985, Reconstructing paleoflood hydrology with slackwater deposits: Verde River, Arizona: M.S. Thesis, Univ. Ariz., Dept. of Geosciences, 48 pp.
- Ely, L.L., and Baker, V.R., 1985, Reconstructing paleoflood hydrology with slackwater deposits: Verde River, Arizona, *Physical Geography*, v. 6, pp. 103-126.
- Ely, L.L., Y. Enzel, V.R. Baker, and D.R. Cayan, 1993, A 5000-year record of extreme floods and climate change in the southwestern United States: *Science*, n. 262, pp. 410-412.

- Ely, L.L., O'Connor, J.E., and Baker, V.R., 1988, Paleoflood hydrology of the Salt and Verde rivers, Central Arizona: in U.S. Committee on Large Dams, 8th Annual Lecture Series, Phoenix, Arizona, pp. 3.1 - 3.35
- Enzel, Y., Ely, L.L., House, P.K., Baker, V.R., and Webb, R.H., 1993, Paleoflood evidence for a natural upper bound to flood magnitudes in the Colorado River Basin: *Water Resources Research*, v. 29, no. 7, pp. 2287-2297.
- Garrett, J.M., and D.J. Gellenbeck, 1991, Basin characteristics and streamflow statistics in Arizona as of 1989: *U.S. Geol. Surv Water Resour. Invest.*, 91-4041, 612 pp.
- Hoggan, D.H., 1989, *Computer-assisted floodplain hydrology and hydraulics*, McGraw-Hill, New York, 518 pp.
- House and Pearthree, in press, A geomorphologic and hydrologic evaluation of an extraordinary flood discharge estimate: Bronco Creek, Arizona: *Water Resources Research*.
- House, P.K., and K.K. Hirschboeck, 1995, Hydroclimatological and paleohydrological context of extreme winter flooding in Arizona, 1993: *Arizona Geological Survey Open-File Report 95-12*, 44 pp.
- Hydrologic Engineering Center, 1985, *HEC-2 water surface profiles users manual*, U.S. Army Corps of Eng., Davis, Calif., 37 pp.
- Kochel, R.C., 1988, Extending stream records with slackwater paleohydrology: examples from west Texas, in *Flood Geomorphology*, edited by V.R. Baker, R.C. Kochel, and P.C. Patton, John Wiley, New York, pp. 377-392.
- Kochel, R.C., and V.R. Baker, 1988, Paleoflood analysis using slackwater deposits, in *Flood Geomorphology*, edited by V.R. Baker, R.C. Kochel, and P.C. Patton, John Wiley, New York, pp. 357-376.
- Lane, W.L., 1987, Paleohydrologic data and flood frequency estimation, in Singh, V.P. ed. *Regional Flood Frequency Analysis*: D. Reidel Publishers, Boston, pp. 287-298.
- Malvick, A.J., 1980, A magnitude-frequency-area relation for floods in Arizona: A study to advance the methodology of assessing the vulnerability of bridges to floods for the Arizona Department of Transportation: *The Engineering Experiment Station, Gen. Rpt. No. 2*, Univ. Ariz. Tucson, 185 pp.
- O'Connor, J.E., and R. H. Webb, 1988, Hydraulic modeling for paleoflood analysis, in *Flood Geomorphology*, edited by V.R. Baker, R.C. Kochel, and P.C. Patton, John Wiley, New York, pp. 393-402.
- O'Connor, J.E., Fuller, J.E., and Baker, V.R., 1986, Late Holocene flooding within the Salt River basin, central Arizona: Unpublished report to the Salt River Project, 84 pp.
- O'Connor, J.E., L.L. Ely, E.E. Wohl, L.E. Stevens, T.E. Melis, V.S. Kale, and V.R. Baker, 1994, A 4500-year record of large floods on the Colorado River in the Grand Canyon, Arizona, *J. Geol.*, n. 102, pp. 1-9.
- Patterson, J.L., and Somers, W.P., 1966, Magnitude and frequency of floods in the United States: Part 9. Colorado River Basin: *U.S. Geological Survey Water-Supply Paper 1683*, 476 pp.
- Roeske, R.H., 1978, Methods for estimating the magnitude and frequency of floods in Arizona: *Arizona Dept. of Transportation Research Project HPR-1-15 (121)*, 82 pp.
- Stedinger, J.R. and Baker, V.R., 1987, Surface water hydrology: historical and paleoflood information: *Reviews of Geophysics*, v. 25, pp. 199-124.

- Stedinger, J.R., and Cohn, T.A., 1986, Flood frequency analysis with historical and paleoflood information: *Water Resources Research*, v. 22, pp. 785-793.
- Stedinger, J., Therivel, R., Grygier, J., Wu, R.S, 1986, Analysis of the frequency of large floods on the Salt and Verde rivers using historical and paleoflood information: Unpublished report to the Salt River Project, Phoenix, Arizona.
- United States Water Resources Council, 1982, Guidelines for determining flood flow frequency, Bulletin 17b of the Hydrology Committee: United States Water Resources Council, Washington, D.C.